Indian Journal of Pure & Applied Physics
Vol. 56, June 2018, pp. 453-460

Hydrothermal synthesis and characterization of nickel doped potassium titanate

Shailendra Rawat[a], Jyotsna Sharma[a] & Shatendra Sharma[b]*

[a]School of Basic and Applied Sciences, K R Mangalam University, Gurugram 122 001, India

[b]University Science Instrumentation Centre, Jawaharlal Nehru University, New Delhi 110 067, India

Received 21 June 2017; accepted 3 November 2017

The potassium titanate nanowires doped with nickel using nickel chloride as dopant are synthesized by hydrothermal method. These synthesized structures are then characterized by XRD, SEM and TEM and the dopant concentrations are estimated by EDS. The XRD characterization of samples shows that the product formed is mainly $K_2Ti_6O_{13}$. The nanowires/fibres of the $K_2Ti_6O_{13}$ are formed having length up to 20 microns and thickness of about 20 nm. The TEM imaging confirms the formation of uniform internal structures of all nanowires however the inner structure of nickel doped samples are denser in comparison to the undoped samples. The annealing of synthesized nanowires at temperatures in the range of 600-1000 °C modifies their crystal structure. The EDS results have shown that the measured Ni doping concentration in all samples is about four times higher than the expected values. Therefore the possibility of chemical bonding or trapping of nickel atoms in the structure cannot be ruled out. The UV-Vis and Raman spectra of the doped samples are compared with that of un-doped samples. In present work, the use of nickel chloride as dopant in potassium titanate using hydrothermal method is reported for the first time.

Keywords: Potassium titanate, Nanowires, Nickel doped, Characterization

1 Introduction

Titanates are one dimensional semi-conducting nano-structures that have remarkable electronic, magnetic, optical, mechanical and catalytic properties which are different from that of their bulk materials. Among these, the potassium titanate is found with several structures like $K_2Ti_2O_5$, $K_2Ti_4O_9$, $K_2Ti_6O_{13}$ and $K_2Ti_8O_{17}$. It is known as a wide band semiconductor with band gap varying from 3.15 to 3.38 eV. The hexa-titanate of potassium ($K_2Ti_6O_{13}$) with a tunnel structure is of great industrial interest due to its thermal stability[1], chemical resistivity, mechanical, dielectric[2] and ion exchange properties[3-15]. Over last few decades it has found versatile applications like hydrolysis[16-20], gas sensing[21], super capacitors and ion-exchange electrodes[22-23]. Potassium titanate nano-tubes and nano-wires are particularly of interest because they have large active surface and may enhance the photo-catalytic activity[24-30], leading to its potential applications in environmental purification, decomposition of carbon acid gas and generation of hydrogen by hydrolysis[22]. Due to the high chemical and thermal stability, the titanate whiskers have found applications in whisker-reinforced plastics and meterials[23]. The potassium titanate has specific photoluminescence and photovoltaic activity that makes it a suitable material for hydrogen evolution via the water splitting reaction even without using co-catalysts[31-33]. The catalytic properties of the titanates have been investigated in detail for their role in the degradation of toxic materials and hydrolysis of pure water owing to their better photo-catalytic properties under UV irradiation, as well for use as an electrode material in sensors[21]. In addition potassium hexa-titananates ($K_2Ti_6O_{13}$, n=6) are widely used as additives to improve the mechanical performance of metals, ceramics and plastics. Due to this property the titanate fibres/whiskers are also used in the manufacture of brake lining of automobiles[34-35]. Many researchers have studied the synthesis and growth of potassium titanate products with different morphology and chemistry. The potassium hexa-titanate can be synthesized by several methods such as calcination[36-39], hydrothermal method[40-49], molten salt synthesis method[50-54] and flux growth[55-56] method. The calcination method is used commercially to produce short fibres or whiskers[13,37,57] with broad size distribution. Hydrothermal synthesis is a one-step, environment friendly and inexpensive method in which the morphology, size and purity of the product can be controlled under moderate conditions[43,48]. Sintering or calcination[36-39], molten salt method[50-54] and

*Corresponding author (E-mail: shatendra@gmail.com)

hydrothermal[40-49] methods are the most popular methods to prepare potassium titanate whiskers. Potassium titanates are crystallized in the form of whiskers at high temperatures in sintering and melting methods. The sintering processes are often complicated and energy consuming as temperatures above 900 °C are required. It is difficult to control the particle size and morphology of products in this process. In order to make the molten salt method more energy efficient, some expensive fluxes are added to lower the melting point of ingredients. These fluxes need to be separated from the final product after process is complete and then recycled. On the other hand, the hydrothermal synthesis is a promising method due to the combined effects of solvent, temperature, and pressure on ionic reaction equilibrium, which can stabilize the desired products while inhibiting the formation of undesirable compounds. Moreover, hydrothermal method yields highly pure, homogeneous whiskers at a considerably lower temperature compared to the solid state reactions in molten salt method. Literature shows that nearly all methods of the hydrothermal synthesis[40-49] of potassium titanates use KOH as potassium source with TiO_2 as titanium source, whereas reaction temperatures and pressures are varied significantly. The method of synthesis and characterization of nickel doped potassium hexa-titanate is not fully explored as very few studies[2,57] on Ni doped $K_2Ti_6O_{13}$ are available in literature. In this paper, we have reported the synthesis and characterization of $K_2Ti_6O_{13}$ using hydrothermal method and it's doping with nickel using $NiCl_2$ as dopant for the first time.

2 Experimental

All chemicals used for the synthesis are procured from Fisher Scientific (anatase TiO_2 molecular weight 79.9), KOH (molecular weight 56.11) and $NiCl_2$. $6H_2O$ (molecular weight 237.69) as dopant. These chemicals are used without any further modification or purification. The calculated molar amounts (by weight) of KOH and nickel chloride are mixed with DI water in a flask and stirred for one hour using a magnetic stirrer. This mixture is labelled as A. In another flask anatase TiO_2 powder is dissolved in 10 mL of pure ethyl alcohol and vigorously stirred for one hour. To this solution 10 mL of DI water is added and stirred further to obtain a homogeneous mixture that is labelled as B. The part A and B of the solutions are mixed together and stirred again for two hours at 60 °C to evaporate ethyl alcohol present in the solution. The mixture is formed like slurry/paste that is transferred to an air tight Teflon lined steel vessel which is placed in an oven at 180 °C for 72 h for synthesis of all samples. After 72 h the oven is switched off and samples are allowed to cool normally to room temperature. The samples are then transferred to glass beaker and thoroughly washed with de-ionized water several times till neutralized to a solution of pH equal to 7.0. The solution is again decanted of clear water and the fibrous structures formed are made to settle down as white product in the beaker. The product is filtered using ample amount of DI water using a vacuum filtration system. All undoped and doped samples are synthesized using the same process except that for doping $NiCl_2$ is also added to the mixture A. All steps of the synthesis process are shown in flowchart (Fig. 1). The synthesized sample powders are then dried at 110 °C in the oven for 24 h before further characterization. In order to observe the effect of annealing on the synthesized samples, some quantities (about 1 g) of each synthesized sample are annealed at 600 °C, 700 °C, 800 °C, 900 °C and 1000 °C for 24 h. The synthesized samples are characterized and the results are discussed in the next section.

3 Results and Discussion

The synthesized samples of potassium titanate are investigated for change in structural (XRD, SEM, TEM) and optical properties (Raman, UV-Vis) of samples due to Ni doping (EDS) and also due to annealing

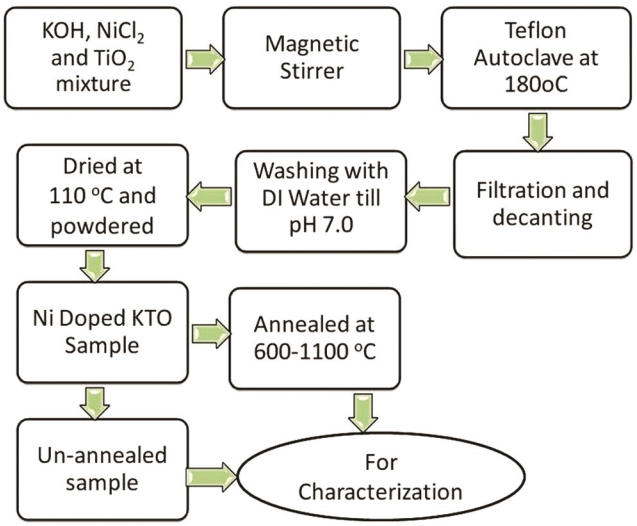

Fig. 1 – Flow chart of the synthesis process used for nickel doped potassium titanate. For undoped samples $NiCl_2$ was not used, rest of the steps remain same.

temperatures varying from 600 °C to 1000 °C. The results are discussed in the following sections.

3.1 X-ray diffraction (XRD)

The XRD measurements are performed using an X-ray diffractometer (model PANalytical Xpert Pro 8). XRD pattern for all samples are recorded at an X-ray wavelength of 1.54 Å of Cu at 2θ steps of 1.5 degree. The X-ray diffraction pattern of un-doped $K_2Ti_6O_{13}$ is shown in Fig. 2 and it perfectly matches with the standard JCPDS data when the peak positions are compared. The XRD pattern for an un-annealed sample of Ni doped $K_2Ti_6O_{13}$ is shown in Fig. 3. The typical XRD pattern for nickel doped and annealed sample of $K_2Ti_6O_{13}$ at 900 °C is shown in Fig. 4. The comparison of 2θ values of XRD peaks of undoped and nickel doped un-annealed and annealed sample (Table 1) shows that there are no overlapping peaks for undoped and doped samples, which indicates that the nickel doping causes some changes in the morphology of the structures. Similarly the annealing of nickel doped sample also shifts some peaks towards lower 2θ values.

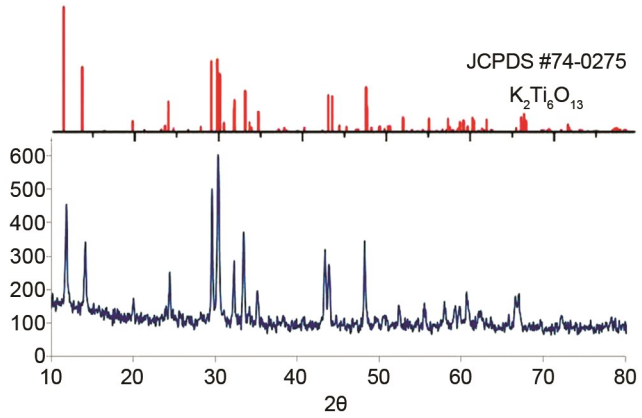

Fig. 2 – X-ray diffraction (XRD) pattern of un-annealed and undoped $K_2Ti_6O_{13}$ sample. The XRD peaks observed in synthesized sample compared with the JCPDS data for $K_2Ti_6O_{13}$ peaks. The peak 2θ values are listed in Table 1.

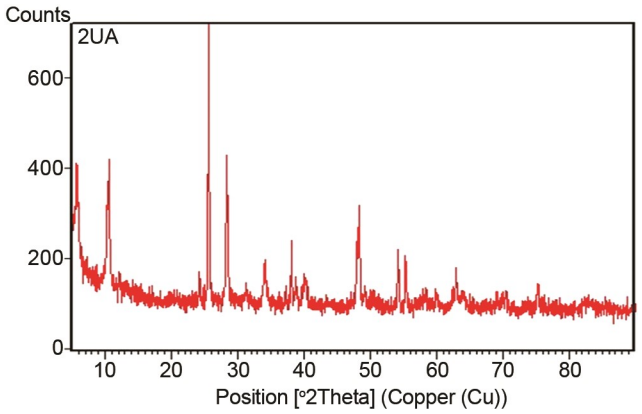

Fig. 3 – X-ray diffraction (XRD) pattern of un-annealed nickel doped $K_2Ti_6O_{13}$. The peak 2θ values are listed in Table 1.

3.2 Scanning electron microscope (SEM) imaging

The surface morphology of the synthesized samples is investigated using a SEM (model

Table 1 – XRD peaks position at 2θ values of un-annealed and annealed samples of $K_2Ti_6O_{13}$.

XRD Peak Positions at 2θ values	Number of peaks	2θ position of the peaks of undoped un-annealed KTO sample (Fig. 2)	2θ position of the peaks of un-annealed Ni doped sample (Fig. 3)	2θ position of the peaks of 900 °C annealed Ni doped sample (Fig. 4)
	1	11.8	5.6	--
	2	14.0	11.5	--
	3	20.0	--	12.5
	4	24.4	--	17.7
	5	29.5	--	25.5
	6	30.3	25.6	--
	7	32.2	--	28
	8	33.3	28.4	--
	9	35.0	34.9	--
	10	43.3	--	36.4
	11	43.8	38.1	--
	12	48.1	--	40.6
	13	52.4	--	48.2
	14	55.4	48.3	--
	15	57.2	54.2	--
	16	59.8	--	54.4
	17	60.7	55.3	--
	18	62.4	--	58.1
	19	66.9	62.9	--
	20	72.2	--	67.1

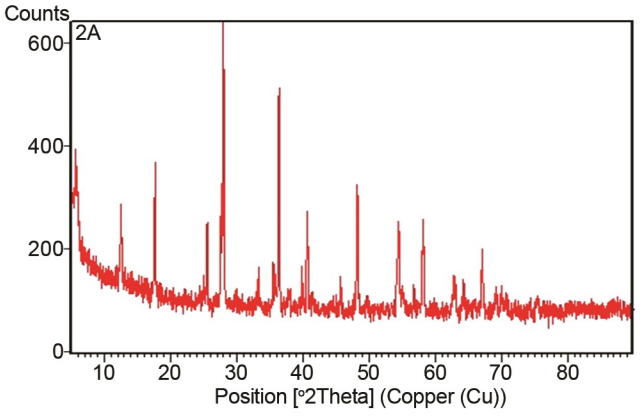

Fig. 4 – X-ray diffraction (XRD) pattern of nickel doped $K_2Ti_6O_{13}$ annealed at 900 °C. The peak 2θ values are listed in Table 1.

Zeiss EVO40). The samples are coated with gold-palladium alloy before performing SEM. The SEM images indicate that the nanowires/fibres of the $K_2Ti_6O_{13}$ are formed with length up to 20 microns and thickness of about 20 nm as shown in Figs 5 and 6. The SEM images also indicate that the nano-wire structure in samples annealed at 800 °C is best as compared to those annealed at other temperatures.

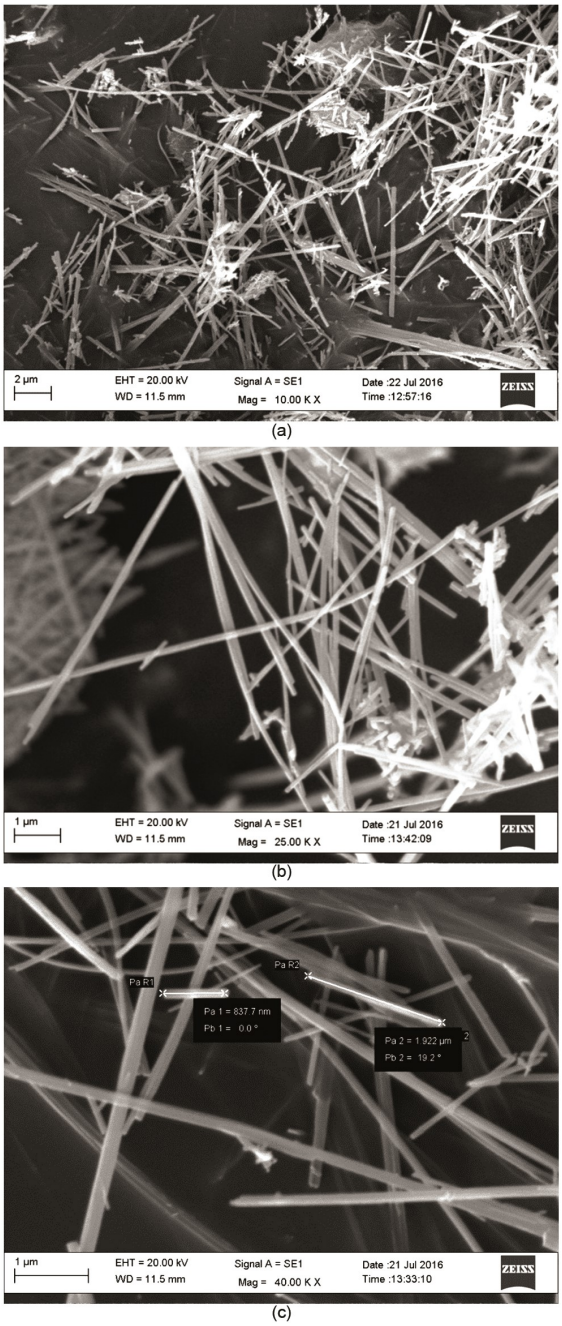

Fig. 5 – Scanning electron microscope (SEM) image of nickel doped $K_2Ti_6O_{13}$ (un-annealed); (a) 10 kx, (b) 25 kx and (c) 40 kx.

3.3 EDS analysis

The EDS analysis on all samples is made to confirm and estimate the extent of doping of Ni in the samples. The energy dispersive spectrometer with Brucker EDS detector attached to SEM (model Zeiss EVO40) is used. The EDS spectra shown in (Fig. 7) confirm the presence of nickel in the synthesized sample. The X-ray spectra show the K-shell X-ray peaks corresponding to oxygen, potassium, titanium

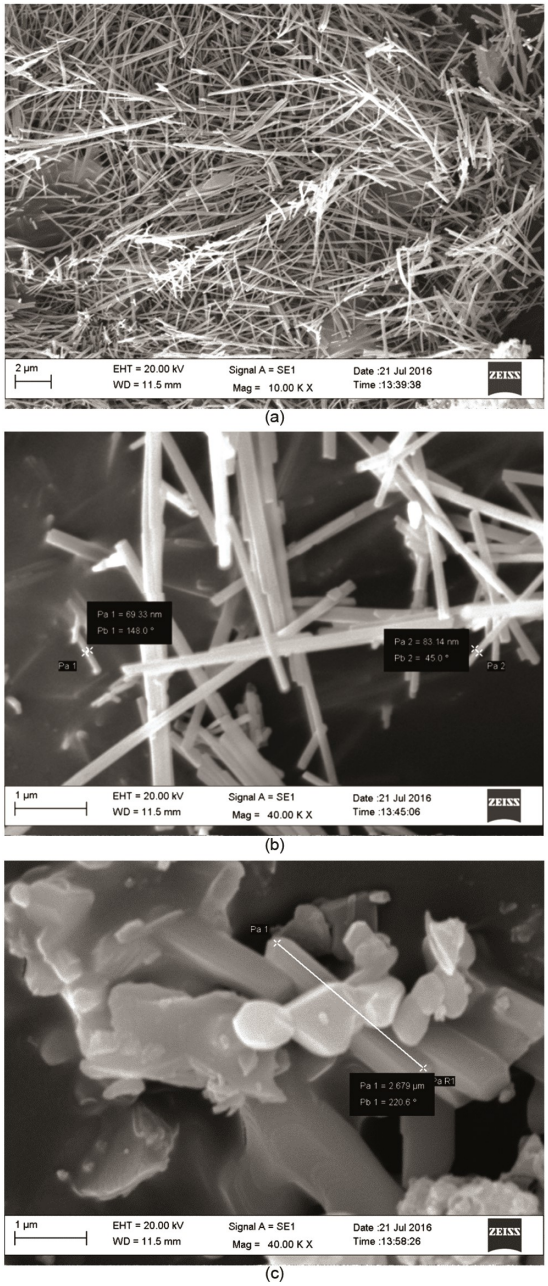

Fig. 6 – Scanning electron microscope (SEM) image of nickel doped $K_2Ti_6O_{13}$ annealed at 800 °C; (a) 10 kx, (b) 25 kx and (c) 40 kx.

and nickel. Since no chlorine K X-ray peak is observed in EDS spectrum, therefore presence of any un-reacted or residual $NiCl_2$ in the sample is completely ruled out. Interestingly, the measured concentration of the Ni in all doped samples is found to be about four times higher than expected. These unexpected concentrations of Ni in doped samples need further investigations.

3.4 Transmission electron microscope (TEM) imaging

TEM imaging of the samples was done using a JEOL 2100F transmission electron microscope. The TEM images of undoped and Ni doped sample of potassium titanate are shown in Fig. 8(a,b). Both images show that the nanowires have a uniform internal structure but vary in lengths. These images also appear to be denser for nickel doped samples as

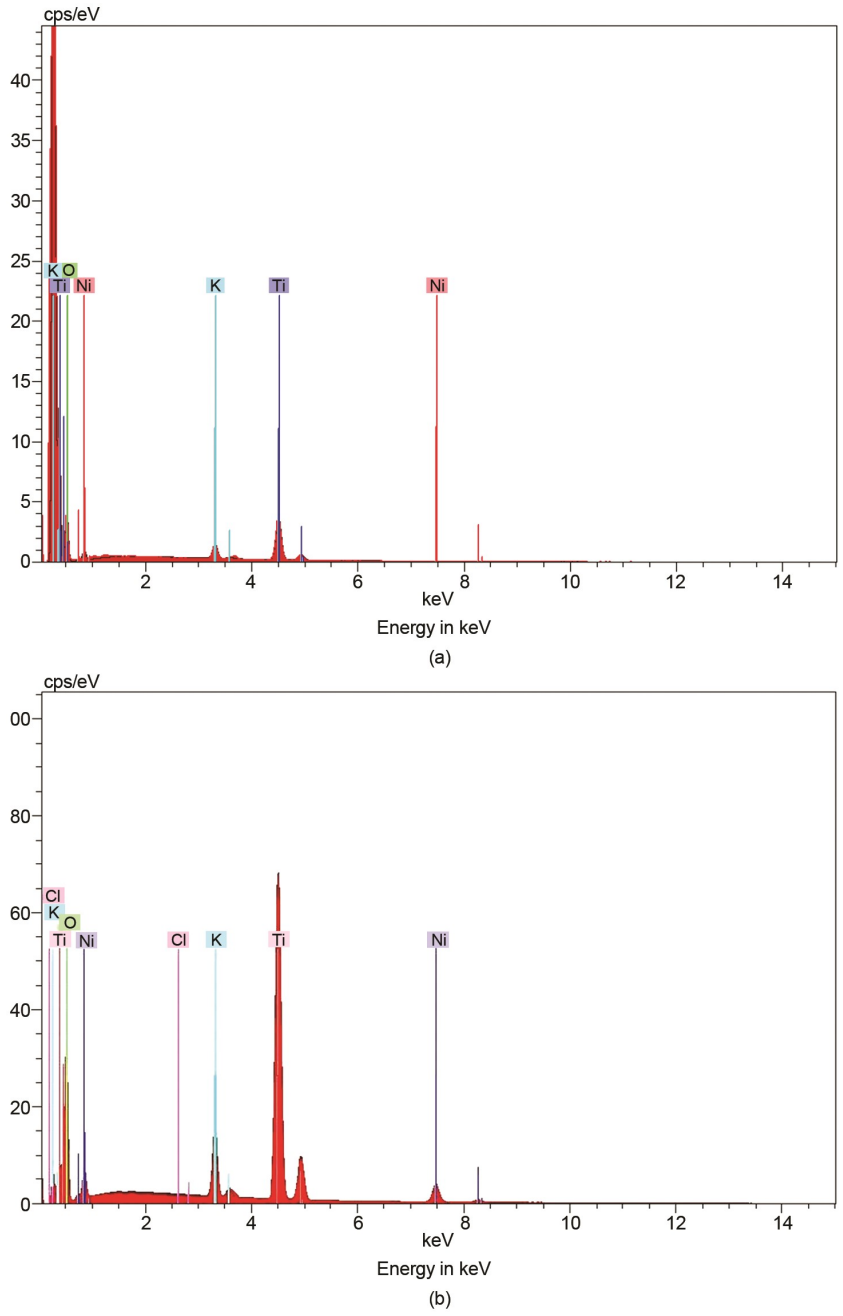

Fig. 7 – Energy dispersive X-ray spectra of (a) undoped and (b) nickel doped $K_2Ti_6O_{13}$. The presence of nickel K X-ray peak in (b) confirms the doping of nickel in the sample. The absence of chlorine X-ray peak in both (a) and (b) indicates that there is no residual $NiCl_2$ in the sample.

compared to the undoped samples. The SAED pattern of nanowires in Fig. 8(c) shows well formed crystal structure of the samples.

3.5 Raman spectrum

The Raman spectrum of un-annealed nickel doped $K_2Ti_6O_{13}$ (Fig. 9) shows well resolved and sharper peaks when compared to the annealed spectra of $K_2Ti_6O_{13}$. This indicates that the annealing at 800 or higher temperatures improves the phase purity of the synthesized sample. It is observed from the spectra that all samples (pure and doped) show similar peaks confirming the formation of pure phase of undoped and nickel doped potassium hexa-titanate (K2Ti6O13) samples.

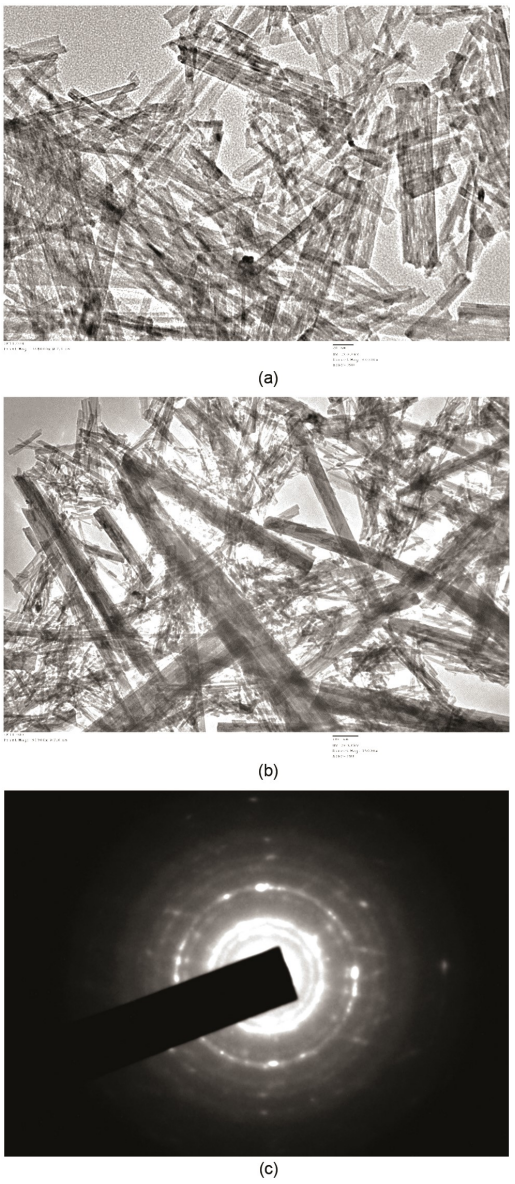

Fig. 8 – TEM images of $K_2Ti_6O_{13}$ synthesized nanowires (a) undoped, (b) Ni doped and (c) SAED pattern of $K_2Ti_6O_{13}$ nanowires. The images show that the nanowires have a uniform internal structure but vary in lengths. Nickel doped structures appear to be more dense inside in comparison to the undoped samples.

3.6 UV-Visible spectra

The optical measurement in UV-Vis region is made on the synthesized samples to get information on the electronic structure of nanowires. The UV-Vis

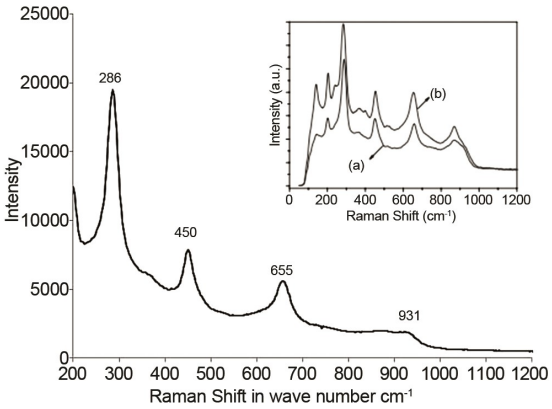

Fig. 9 – Raman spectrum of synthesized $K_2Ti_6O_{13}$. The Raman peaks of synthesized sample match with those reported by other workers-inset (Meng *et al.*[43]).

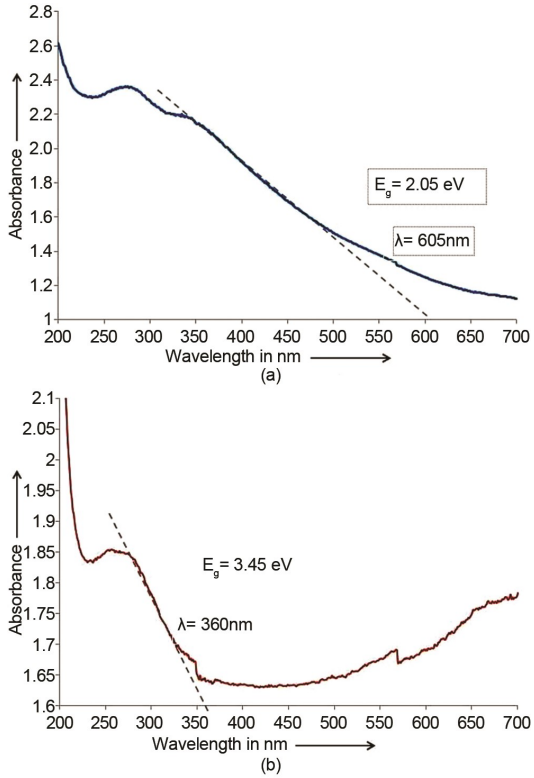

Fig. 10 – UV-Visible spectra of synthesized $K_2Ti_6O_{13}$ samples (a) undoped and (b) nickel doped. The energy band gap is calculated using E_g= 1240.82/ λ.

spectrum of the synthesized sample in the form of a fine powder in DI water solution is recorded using an UV-Vis (P G Instruments Ltd) spectrophotometer (Fig. 10). The UV–Vis absorption spectrum of the $K_2Ti_6O_{13}$ nanowires shows a strong absorption in the ultraviolet region with peaks at 280 nm and 345 nm in undoped sample. A comparison of the UV-Vis spectrum of our sample with those available in the literature[20,43,56] confirms the formation of the $K_2Ti_6O_{13}$ phase of the potassium titanate. It is also observed that these absorption maxima at 280 nm turns to a platau in the range of 245 nm to 278 nm with Ni doping and the maxima at 345 nm disappears in case of nickel doped sample. The λ_{onset} of the spectrum recorded from the nickel doped samples is about 360 nm corresponding to a band gap of 3.45 eV, and for undoped sample it is 605 nm corresponding to a band gap of 2.05 eV which is close to the value reported. When compared with the undoped $K_2Ti_6O_{13}$ nanowires, the spectrum of the nickel doped $K_2Ti_6O_{13}$ nanowires showed stronger absorption in the ultraviolet as well visible region.

4 Conclusions

Hydrothermal synthesis of well formed $K_2Ti_6O_{13}$ nanowires of thickness in the range of 20-50 nm and length up to 200 μm is carried using anatase TiO_2 as precursor. The doping of Ni in $K_2Ti_6O_{13}$ has been successfully carried out using hydrothermal method with nickel chloride as one of the reactant. The influence of doping and annealing on the characteristic properties of $K_2Ti_6O_{13}$ is also investigated using XRD, SEM, EDS, TEM, Raman and UV-Visible techniques. The UV–Vis absorption spectrum of the $K_2Ti_6O_{13}$ nanowires shows a strong absorption in the ultraviolet region. The attained doping concentrations in the sample are also verified by EDS. It is observed that a higher than expected percentage of Ni is present in the samples. This can be attributed to the possible surface or chemical bonding of nickel at some positions or defects apart from the doping. A further investigation to this anomalous concentration of Ni is required.

Acknowledgement

The financial assistance under UPOE-II project by Jawaharlal Nehru University, New Delhi-110067, India is gratefully acknowledged.

References

1 Bamberger G M, *Appl Spectrosc*, 44 (1990) 30.
2 Siddiqui A M, Chandel V S, Shariq M & Azam A, *J Mater Sci Mater Electron*, 24 (2013) 4725.
3 Zhang H X, He X D & He F, *J Alloys Compd*, 472 (2009) 194.
4 Martel R, Schmidt T, Shea H R, Hertel T & Avouris P, *Appl Phys Lett*, 73 (1998) 2447.
5 Bachtold A, Hadley P, Nakanishi T & Dekker C, *Science*, 294 (2001) 1317.
6 Zhang X K, Tang S L, Zhai L, Yu J Y, Shi Y G & Du Y W, *Mater Lett*, 63 (2009) 887.
7 Kang S O, Jang H S, Kim K I, Kim K B & Jung M J, *Mater Lett*, 61 (2007) 473.
8 Kim Y C, Cho M H, Kim S J & Jang H, *Wear*, 264 (2008) 204.
9 Bavykin D V & Walsh F C, *J Phys Chem C*, 111 (2007) 14644.
10 Kim T W, Kim I Y, Im J H, Ha H W & Hwang S J, *J Photochem Photobiol A: Chem*, 205 (2009) 173.
11 Huang M H, Mao S, Feick H, Yan H, Wu Y, Y Kind H, Weber E, Russo R & Yang P, *Science*, 292 (2001) 1897.
12 Ramirez J & Fabry P, *Sens Actuators B*, 77 (2001) 339.
13 Lu J Z & Lu X H, *J Appl Polym Sci*, 82 (2001) 368.
14 Wu S Q, Wei Z S & Tjong S C, *Compos Sci Technol*, 60 (2000) 2873.
15 Zhanga A, Zhaoa G, Huia Y & Guan Y, *Polym Plast Technol Eng*, 56 (2017) 382.
16 Park J, *J Alloys Compd*, 492 (2010) 57.
17 Zhang X K, Yuan J J, Yu H J, Zhu X R, Yin Z & Shen H, *J Alloys Compd*, 631 (2015) 171.
18 Zhen L, Xu C Y, Wang W S, Lao C S & Kuang Q, *Appl Surf Sci*, 255 (2009) 4149.
19 Štengl V, Bakardjieva S, Šubrt J, Većernikova E, Szatmary L, Klementova M & Balek V, *Appl Catal B: Environ*, 63 (2006) 20.
20 Siddiqui M A, Chandel V S & Azam A, *Appl Surf Sci*, 258 (2012) 7357.
21 Burmistrov I N, Varezhnikov A S, Musatov V Y, Lashkov A V, Gorokhovsky A V, Yudinceva T I & Sysoea V V, *IEEE*, 978-1-4799 (2015) 8203.
22 Zhou W, Liu X, Sang Y, Zhao Z, Zhou K & Liu H, *Appl Mater Interfaces*, 6 (2014) 4578.
23 Wang Q, Zhanhu G & Jong S C, *Mater Res Bulletin*, 44 (2009) 1973.
24 Zhang X K, Tang S L, Zhai L, Yu J Y, Shi Y G & Du Y W, *Mater Lett*, 63 (2009) 887.
25 Kang S O, Jang H S, Kim K I, Kim K B & Jung M J, *Mater Lett*, 61 (2007) 473.
26 Kim Y C, Cho M H, Kim S J & Jang H, *Wear*, 264 (2008) 204.
27 Lu J Z & Lu X H, *J Appl Polym Sci*, 82 (2001) 368.
28 Zhang H X, He X D & He F, *J Alloys Compd*, 472 (2009) 194.
29 Bavykin D V & Walsh F C, *J Phys Chem C*, 111 (2007) 14644.
30 Kim T W, Kim I Y, Im J H, Ha H W & Hwang S J, *J Photochem Photobiol A Chem*, 205 (2009) 173.
31 Inoue Y, Kubokawa T & Sato K, *J Chem Soc Chem Commun*, (1990) 1298.
32 Ogura S, Kohno M, Sato K & Inoue Y, *Phys Chem Chem Phys*, 1 (1999) 179.
33 Ogura S, Kohno M, Sato K & Inoue Y, *Appl Surf Sci*, 121 (1997) 521.
34 Halberstadt M L & Rhee S K, *Wear*, 46 (1978) 109.

35 Mahale V, Bijwe J & Sinha S, *Wear*, 376 (2017) 727.
36 Liu C Y, Yin H B, Liu Y M, Ren M, Wang A L, Ge C, Yao H P, Feng H, Chen J & Jiang T S, *Mater Res Bull*, 44 (2009) 1173.
37 Bao N, Shen L, Feng X & Lu X, *J Am Ceram Soc*, 87 (2004) 326.
38 Wang Q, Guo Z & Chung J S, *Mater Res Bull*, 44 (2009) 1973.
39 Lu J Z & Lu X H, *J Appl Polym Sci*, 82 (2001) 368.
40 Hakuta Y, Hayashi H & Arai K, *J Mater Sci*, 39 (2004) 4977.
41 Zhang T, Chen Q & Peng L M, *Adv Funct Mater*, 18 (2008) 3018.
42 Wang B L, Chen Q, Wang R H & Peng L M, *Chem Phys Lett*, 376 (2003) 726.
43 Meng X D, Wang D Z, Liu J H, Lin B X & Fu Z X, *Solid State Commun*, 137 (2006) 146.
44 Wang B L, Chen Q, Hu J, Li H, Hu Y F & Peng L M, *Chem Phys Lett*, 406 (2005) 95.
45 Xiangdong M, Dazhi W, Jinhua L, Bixia L & Zhuxi F, *Solid State Commun*, 137 (2006) 146.
46 Yahyaa R, Hassan A & Aiyub Z, *Mater Sci Forum*, 517 (2006) 222.
47 Shimizu T & Morita T, *J Ceram Soc Jpn*, 85 (1977) 189.
48 Yuan Z Y, Zhang X B & Su B, *Appl Phys*, 78 (2004) 1063.
49 Kapusuz D, Kalay E Y, Park J & Qzturk A, *J Ceram Process Res*, 16 (2015) 291.
50 Teshima K, Yubuta K, Shimodaira T, Suzuki T, Endo M, Shishido T & Oishi S, *Cryst Growth Des*, 8 (2008) 465.
51 Xu C Y, Zhang Q, Zhang H, Zhen L, Tang J & Qin L C, *J Am Chem Soc*, 127 (2005) 11584.
52 Xu L Q & Cheng L, *Mater Charact*, 61 (2010) 245.
53 Suzuki S, Teshima K, Kiyohara M, Kamikawa H, Yubuta K, Shishido T & Oishi S, *Cryst Eng Commun*, 14 (2012) 4176.
54 Zaremba T, *Mater Sci Poland*, 30 (2012) 180.
55 Suzuki S, Teshima K, Kiyohara M, Kamikawa H, Yubuta K, Shishido T & Oishi S, *Cryst Eng Commun*, 14 (2012) 4176.
56 Lianqiang X & Li C, *Mater Charact*, 61 (2010) 245.
57 Gao T, Norby P, Okamoto H & Fjellvag H, *Inroga Chem*, 48 (2009) 9409.